Coprime Visible Regions Assisted Angle Unfolding for Sparse ESPRIT

Lifan Xu and Shunqiao Sun
Department of Electrical and Computer Engineering
The University of Alabama, Tuscaloosa, AL, USA

***Abstract*—In many applications, such as automotive radar for autonomous vehicles, a sparse linear array (SLA) is more attractive than a uniform linear array (ULA). SLAs not only make hardware costs lower to design antenna arrays with a large aperture but also reduce the mutual coupling among antenna elements. When estimation of signal parameters via rational invariance techniques (ESPRIT) is applied on SLAs with shift among subarrays being larger than half wavelength, there would be ambiguities in the field of view (FoV) of the sensor array due to angle folding. In this paper, we present novel SLA geometry with non-uniform subarrays that do not necessarily have a centrally symmetric geometry, and corresponding coprime FoV aided approach to do the angle unfolding. The main goal of the sparse array design is to increase the array aperture size using fewer sensors while maintaining shift invariant geometry. By carefully designing the shifts among these sparse subarrays following a coprime relationship, the angles can be resolved uniquely by a consistent comparison of the angle estimations reported separately by different shifted subarrays.**

***Index Terms*—Coprime visible regions, angle estimation, sparse array, ESPRIT, unfolding**

I. Introduction

The direction of arrival (DoA) estimation of multiple targets using a set of sensors has been widely discussed in the literature. For a standard uniform linear array (ULA) with element spacing of half wavelength, digital beamforming (DBF) [1] techniques can find angles of the targets without ambiguity by applying the fast Fourier Transform (FFT) to snapshots across all the sensors. Although DBF can efficiently be implemented even with a single snapshot in embedded digital signal processing systems, for a given array aperture size, the resolution of DBF is limited by FFT. Subspace-based super-resolution algorithms have been developed. For example, multiple signal classification (MUSIC) exploits the orthogonality between signal space and noise space to obtain the pseudo-spectrum [2]. Usually, fine discrete fine grids are required in MUSIC, which results in high computational cost. The root-MUSIC [3] is the variation of MUSIC which solves a polynomial rooting problem and avoids grid search. Multiple snapshots are required of classical MUSIC to estimate signal and noise spaces accurately. A single snapshot MUSIC was proposed in [4], which exploited the noise subspace of a Hankel matrix constructed via spatial smoothing of the single array snapshot. Another classical and popular subspace-based angle estimation algorithm for ULA is ESPRIT [5], which exploits the phase shifting information among identical subarrays. ESPRIT avoids grid search and thus is more computationally efficient than MUSIC. To further reduce the ESPRIT computation complexity for a larger array, beamspace ESPRIT was proposed in [6] to resolve angle in parallel with high resolution and accuracy by reducing the dimension of the covariance matrix with sophisticated transformation matrices, e.g., Discrete Fourier transform (DFT) transformation matrix. Different from the rank-revealing factorizations of complex-valued matrices in the original ESPRIT, unitary ESPRIT [7] utilizes unitary transformation to form real-valued matrices to reduce computational burden.

In many applications, such as automotive radar for autonomous vehicles [8]–[11], a sparse linear array (SLA) is more attractive than a ULA. Sparse linear arrays not only make hardware costs lower to design antenna arrays with a large aperture but also reduce the mutual coupling among antenna elements. For ULA with half-wavelength interelement spacing, the aperture is proportional to the number of array sensors. Thus, a high number of antennas is requied for high-resolution DoA estimation, which are often infeasible in automotive radar applications due to the strict cost constraints. Multiple-input multi-output (MIMO) radar [12] has been introduced to design automotive radar to achieve a large virtual aperture at a low cost [8]. However, the cost of synthesizing a large virtual ULA with half-wavelength interelement spacing using MIMO radar technology remains high. To further reduce the cost without sacrificing the high angular resolution is via the use of nonuniform, or sparse linear arrays (SLAs) [13], [14]. For a certain aperture size, a SLA has much fewer elements than a ULA. However, performing DBF along an SLA results in high sidelobes and even grating lobes which would make angle finding fail. To suppress unwanted spurious peaks in the beampattern, it is common to interpolate the missing elements of SLA. Transformation matrix is proposed in [15] to interpolate the SLA. Matrix completion methodology was studied in [16], [17] to fill the holes in the SLA, and in [18]–[20] the coprime and nested structures were investigated to obtain an enhanced ULA. After interpolation, DBF can be utilized in the interpolated array for angle finding. Unlike the interpolation methods, compressive sensing (CS) [21] and the iterative adaptive approach (IAA) [22] can be directly implemented for angle finding with SLAs. However, they have high computational costs and the number of angles that can be resolved should be sparse for CS. Artificial intelligence

This work was supported in part by U.S. National Science Foundation (NSF) under Grant CCF-2153386 and Alabama Transportation Institute (ATI).

2023 IEEE Radar Conference (RadarConf23) | 978-1-6654-3669-4/23/$31.00 ©2023 IEEE | DOI: 10.1109/RADARCONF2351548.2023.10149628

techniques can also be applied for DoA estimation with SLAs [23]. But DoA estimation using deep neural networks suffers from generalization issue. It is also possible to apply subspace methods, e.g., MUSIC and ESPRIT, for sparse linear arrays, if the array geometry matches the unambiguous requirement [24]. Directly applying the ESPRIT method in the sparse array is attractive due to the low computational complexity compared with MUSIC. However, for ESPRIT, when the shifting among subarrays is larger than half wavelength, there will be angle aliasing in the field of view (FoV), which introduces ambiguities, i.e., false estimations.

In this paper, we present a sparse array geometry design and corresponding unfolding ESPRIT algorithm to resolve ambiguous angles. The sparse array consists of three identical sparse subarrays with different shift invariant structures that are much larger than half wavelength to achieve a large antenna array aperture. By carefully designing the shifts among these sparse subarrays following a coprime relationship, the DoA can be resolved uniquely by a consistent comparison of the DoA estimation reported separately by the three coprime FoVs.

Throughout this paper, matrices and vectors are represented in upper and lower case bold, respectively. The conjugate transpose is $(\cdot)^H$ and the complex values set is $\mathbb{C}$. The notation "$\cdot$" denotes the dot product, and the expectation operator is $E\{\cdot\}$.

II. System Model

Consider K narrow band noncoherent signals impinging on a ULA with N sensors deployed along the x axis with element spacing d. The received signal at snapshot t is given by

$$\mathbf{y}(t) = \sum_{k=1}^{K} \mathbf{a}(\theta_k) s_k(t) + \mathbf{n}(t), \tag{1}$$

where the s_k denotes the radar cross section of the k-th target, and the additive noise vector $\mathbf{n}(t)$ at the t-th snapshot is independent from sources and is assumed to be zero-mean white Gaussian noise with variance σ^2. The array steering vector has the form as

$$\mathbf{a}(\theta_k) = \left[1, e^{-j2\pi d/\lambda \sin(\theta_k)}, \cdots, e^{-j2\pi(N-1)d/\lambda \sin(\theta_k)}\right]^T. \tag{2}$$

The output of a SLA with N_s elements ($N_s < N$) is part of the ULA output, and its data can be defined by a mask vector $\mathbf{m} = [u_1, u_2, \cdots, u_N]^T$ where the element u_i represents the state of the i-th sensor of the ULA. If $u_i = 1$, the i-th element exists in the SLA. If $u_i = 0$, the i-th element is a hole in the SLA.

To simplify formulation, we fix the two sensors at both ends to maintain the same array aperture as the ULA and select $N_s - 2$ other sensors in-between, rendering a SLA with total of N_s sensors. It holds that trace $\mathrm{tr}\{\mathbf{m}\mathbf{m}^T\} = N_s$. By carefully designing the mask vector $\mathbf{m}$, it is possible to form

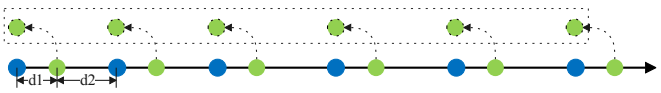

Fig. 1. The illustration of a staggered array [26].

SLAs that contain identical subarrays. The t-th snapshot array output of a SLA is given as

$$\mathbf{y}_s(t) = \mathbf{y}(t) \odot \mathbf{m}, \tag{3}$$

where $\odot$ denotes element-wise multiplication. The output vector $\mathbf{y}_s(t)$ also has a dimension $\mathbb{C}^{N\times 1}$, which means that it is not a compact form and the missing element has been filled in with "0".

We consider to utilize ESPRIT to carry out DoA estimation for SLAs. The basic assumption of ESPRIT is that the two subarrays overlap completely after shifting a subarray a certain distance Δ along the direction of sensor deployment. The relationship between the DoA estimation error variance, shift distance Δ, and the number of elements in a subarray, N_{cs}, has been investigated in [25]. It is shown that with the value of N_{cs} and Δ increasing, the DoA estimation error decreases. However, the visible region of ESPRIT is confined by the following relation

$$-\pi \le 2\pi|\Delta|\sin(\theta_k) \le \pi. \tag{4}$$

A visible region of $[-\pi/2,\ \pi/2]$ renders the shift distance $\Delta \le \lambda/2$. Once the shift is larger than $\lambda/2$, there would be grating lobes in the visible region, resulting in ambiguities in DoA estimation. For ULA subarrays, a two-step procedure was proposed in [25] to decrease DoA estimation error by using larger Δ. This method first estimates the angle with a small Δ and then switches to a larger Δ to further decrease the estimation error. A SLA with paired staggered ULA subarrays was proposed in [26] to do angle finding. An example of staggered array is shown in Fig. 1, where the SLA consists of two ULA subarrays with elements spacing $d_1 + d_2$ and the two identical subarrays are shifted by d_1. The staggered arrays listed in Fig. 1 can be viewed as a uniform rectangular array (URA) with two layers, by virtually treating the green subarray as the top layer of the URA. By choosing values of d_1 and d_2 as a coprime pair, two-dimensional unitary ESPRIT can be used to find DoA without ambiguity. However, this approach requires a SLA with centrally symmetric geometry so that the unitary ESPRIT can be applied.

III. Coprime FoV Aided Sparse Array Design

In this paper, we consider the visible region as $[-\pi/2,\ \pi/2]$. We present a coprime FoV method to do the angle unfolding for SLAs with non-uniform subarrays which do not necessarily have a centrally symmetric geometry. The main goal of the sparse array design is to increase the array aperture size using fewer sensors while maintaining shift invariant geometry. To achieve the large antenna array aperture, a large Δ is expected.

A. ESPRIT On Sparse Linear Arrays

We propose a sparse array design that consists of three identical sparse subarrays. Let zero-filled sparse vectors $\mathbf{y}_{s1}(t)$, $\mathbf{y}_{s2}(t)$ and $\mathbf{y}_{s3}(t)$ denote the outputs of the three sparse subarrays and they can be expressed as

$$\begin{aligned}
\mathbf{y}_{s1}(t) &= \sum_{k=1}^{K} \tilde{\mathbf{a}}(\theta_k) s_k(t) + \mathbf{n}_1(t) = \mathbf{A}\mathbf{s}(t) + \mathbf{n}_1(t) \\
\mathbf{y}_{s2}(t) &= \sum_{k=1}^{K} \tilde{\mathbf{a}}(\theta_k) s_k(t) e^{j\phi_k} + \mathbf{n}_2(t) = \mathbf{A}\mathbf{\Phi}\mathbf{s}(t) + \mathbf{n}_2(t), \\
\mathbf{y}_{s3}(t) &= \sum_{k=1}^{K} \tilde{\mathbf{a}}(\theta_k) s_k(t) e^{j\psi_k} + \mathbf{n}_2(t) = \mathbf{A}\mathbf{\Psi}\mathbf{s}(t) + \mathbf{n}_3(t),
\end{aligned} \tag{5}$$

where $\tilde{\mathbf{a}}(\theta_k)$ is a subset of $\mathbf{a}(\theta_k)s_k(t)\cdot\mathbf{m}$. The array manifold is represented as $\mathbf{A} = [\tilde{\mathbf{a}}(\theta_1), \tilde{\mathbf{a}}(\theta_2), \cdots, \tilde{\mathbf{a}}(\theta_K)] \in \mathbb{C}^{N_{ms}\times K}$, where N_{ms} denotes the number of element positions in the subarray (including the hole positions). The phase shifts among the three subarrays are denoted as $e^{j\phi}$ and $e^{j\psi}$, respectively. The diagonal matrices $\mathbf{\Phi}$ and $\mathbf{\Psi}$ contain the phase shifts with respect to K targets, i.e.,

$$\mathbf{\Phi} = \text{diag}\left(\left[e^{j\phi_1}, e^{j\phi_2}, \cdots, e^{j\phi_K}\right]\right), \tag{6}$$

$$\mathbf{\Psi} = \text{diag}\left(\left[e^{j\psi_1}, e^{j\psi_2}, \cdots, e^{j\psi_K}\right]\right). \tag{7}$$

Here, $\mathbf{s}(t) = [s_1(t),\ s_2(t),\ ...,\ s_K(t)]^T$ is the signal vector. Since the multiplication of zero-filled rows in $\mathbf{A}$ with $\mathbf{\Phi}$ or $\mathbf{\Psi}$ are still zeros, the phase shifts at zero-filled positions are unnecessary, as they do not provide any information. Therefore, in the following of this paper, compact array measurement vector obtained by removing the zeros corresponding to holes in the subarrays, is used to save storage space. For example, the stacked subarrays 1 and 2 measurement vector in the compact form is given by

$$\mathbf{y}_{c1}(t) = \begin{bmatrix} \mathbf{A}_c \\ \mathbf{A}_c\mathbf{\Phi} \end{bmatrix} \mathbf{s}(t) + \mathbf{n}(t) = \mathbf{P}\mathbf{s}(t) + \mathbf{n}(t), \tag{8}$$

where $\mathbf{y}_{c1}(t)$ and $\mathbf{A}_c$ are all in the compact form. The dimension of the ESPRIT steering matrix $\mathbf{P}$ is $\mathbb{C}^{2N_{cs}\times K}$, where N_{cs} is the number of elements in a subarray.

Assume that there are L snapshots available to estimate DoA, i.e., $\mathbf{Y}_c = [\mathbf{y}_c(1), \cdots, \mathbf{y}_c(L)]$. The sampling covariance matrix is expressed as

$$\hat{\mathbf{R}}_{c1} = \frac{1}{L}\sum_{t=1}^{L} \mathbf{y}_{c1}(t)\, \mathbf{y}_{c1}^H(t). \tag{9}$$

After performing eigenvalue decomposition on $\hat{\mathbf{R}}_{c1}$, we have the following structure

$$\hat{\mathbf{R}}_{c1} = \sum_{i=1}^{2N_{cs}} \lambda_i \mathbf{e}_i \mathbf{e}_i^H, \tag{10}$$

Assume that the number of target K is less than the sensor elements in the subarray, i.e., $K < N_{cs}$. The eigenvectors and eigenvalues corresponding to K targets are arranged into a signal-related matrix $\mathbf{E}_s$ and a diagonal eigenvalue matrix $\mathbf{\Lambda}$ in sorted order, respectively. The noise matrix is represented as $\mathbf{E}_n \in \mathbb{C}^{2N_{cs}\times(2N_{cs}-K)}$ and its corresponding eigenvalue matrix is $\mathbf{\Lambda}_n$. Therefore, the eigenvalue decomposition of $\hat{\mathbf{R}}_{c1}$ can be written as summation of signal and noise parts, i.e.,

$$\hat{\mathbf{R}}_{c1} = \mathbf{E}_s\mathbf{\Lambda}_s\mathbf{E}_s^H + \mathbf{E}_n\mathbf{\Lambda}_n\mathbf{E}_n^H, \tag{11}$$

This partition indicates that the rank of signal space is equal to the rank of the steering matrix, i.e., $\text{rank}(\mathbf{E}_s) = \text{rank}(\mathbf{P})$. Thus, there is a unique nonsingular matrix $\mathbf{U}$ such that

$$\mathbf{E}_s = \mathbf{P}\mathbf{U}, \tag{12}$$

or equivalently

$$\begin{bmatrix} \mathbf{E}_{\text{s1}} \\ \mathbf{E}_{\text{s2}} \end{bmatrix} = \begin{bmatrix} \mathbf{A}_c\mathbf{U} \\ \mathbf{A}_c\mathbf{\Phi}\mathbf{U} \end{bmatrix}. \tag{13}$$

Since $\mathbf{E}_{\text{s1}} \in \mathbb{C}^{N_{cs}\times K}$ and $\mathbf{E}_{\text{s2}} \in \mathbb{C}^{N_{cs}\times K}$ have the same column space, and therefore the estimated phase shift matrix, $\hat{\mathbf{\Phi}}$, lies in the eigenvalues of the following matrix $\mathbf{T} \in \mathbb{C}^{K\times K}$ obtained via a least square approach, shown below

$$\mathbf{T} = \left(\mathbf{E}_{\text{s2}}^H\mathbf{E}_{\text{s2}}\right)^{-1}\mathbf{E}_{\text{s2}}^H\mathbf{E}_{\text{s1}}. \tag{14}$$

The k-th DoA estimation can be obtained as

$$\hat{\theta}_k = \text{asin}\left(\frac{\hat{\phi}_k}{2\pi|\Delta_1|}\right). \tag{15}$$

In a similar way, the sampling covariance matrices $\hat{\mathbf{R}}_{c2}$ and $\hat{\mathbf{R}}_{c3}$, corresponding to stacking subrray 1 and subrray 3 with shift of Δ_2, stacking subrray 2 and subrray 3 with shift of Δ_3, can be obtained, respectively. Then, the other two groups of DoA estimations can be computed following the above procedure.

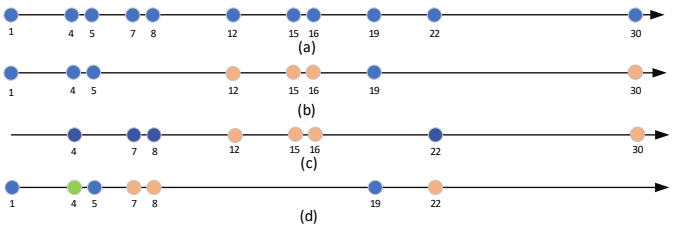

Fig. 2. (a) The proposed coprime FoV sparse linear array; (b-d) Illustration of three possible combinations of shifted subarrays. The green dots denote the sharing elements by two subarrays.

B. Angle Unfolding With Coprime FoV

The equation (4) indicates that the arrival angle of targets beyond the visible region will be folded into narrow FoV and result in false detections for a large Δ. To solve this issue, other subarrays are required to form different folded angle sets. Fig. 2 illustrates an example of coprime FoV sparse array, where the coprime FoV array consists of three shift invariant subarrays, located on gird with indices of $[1, 4, 5, 19]$, $[12, 15, 16, 30]$, and $[4, 7, 8, 22]$. Here, one grid size represents half wavelength. Different shift invariant subarrays combinations with different shifts are shown in Fig. 2 (b)-(d), where

green dots represent the duplicated sensors that are shared by two subarrays. The shifts among all the two groups of subarrays are $\Delta_1 = 5.5\lambda$ (see Fig. 2 (b)), $\Delta_2 = 4\lambda$ (see Fig. 2 (c)), and $\Delta_3 = 1.5\lambda$ (see Fig. 2 (d)). These shifts follow a coprime relationship. Coprime yields different FoVs, as a result of which the angles can be uniquely identified.

To obtain three different subarray sets while using fewer sensors, some of the sensors should be shared by different subarrays. The relationship between FoV and Δ in (4) implies that the shifts Δ_i and Δ_j should satisfy: 1) yield coprime FoVs; 2) the difference of Δ_i and Δ_j is large enough, especially when Δ_i and Δ_j are large numbers. For example, if the shift Δ_i and Δ_j are 5λ and 5.5λ, the corresponding FoVs are $[-5.73^\circ,\ 5.73^\circ]$ and $[-5.21^\circ,\ 5.21^\circ]$, respectively. These small differences in FoV sets result in folded angles that are close to each other and therefore it is not easy to tell the correct DoAs from the ambiguities.

The number of targets K in the array output data needs to be known, which can be estimated with many algorithms, e.g., the Akaike information criterion (AIC) [27], minimum description length (MDL) principle [28] and random matrix theory method (RMT) [29]. The number of ambiguities of one target is $2\Delta_i$, including the true target. The solution sets $\mathbf{D}_1 = [\mathbf{d}_1^1, \cdots, \mathbf{d}_K^1]$, $\mathbf{D}_2 = [\mathbf{d}_1^2, \cdots, \mathbf{d}_K^2]$ and $\mathbf{D}_3 = [\mathbf{d}_1^3, \cdots, \mathbf{d}_K^3]$ estimated via ESPRIT using the three group subarrays are used to carry out a consistency check. This check is a column-to-column comparison and each column only contains a single correct target solution. Therefore, the minimum difference solution of all sets would be chosen as the final angle estimation. In practice, the noise level does affect the subarray estimation accuracy, and the different values of Δ provide slightly different estimation results. Therefore, the consistent results in the three solution sets will be taken as the mean value. The targets obtained by consistency comparison and averaging between the three solution sets are denoted as $\hat{\theta}_k$ for $k = 1, \cdots, K$. Algorithm 1 summarizes these steps of the proposed coprime FoV array angle unfolding for sparse ESPRIT (CoFoV-SESPRIT).

Algorithm 1: Coprime FoV Array Angle Unfolding for Sparse ESPRIT (CoFoV-SESPRIT)

Data: $K,\ L,\ \hat{\mathbf{Y}}_s,\ \Delta_1,\ \Delta_2,\ \Delta_3$
Result: $\hat{\theta} = \left[\hat{\theta}_1, ..., \hat{\theta}_K\right]$
while $i \leq 3$ **do**
  $\hat{\mathbf{R}}_{ci} = \frac{1}{L}\sum_{t=1}^{L} \mathbf{y}_{ci}(t)\hat{\mathbf{y}}_{ci}^H(t)$,
  Do eigendecomposition of $\hat{\mathbf{R}}_{\mathrm{ci}}$,
  Find $\hat{\mathbf{\Phi}}$ or $\hat{\mathbf{\Psi}}$,
  Get solution set $\mathbf{D}_i$,
end
while $k \leq K$ **do**
  $\mathrm{ind}_k = \min_k(\mathrm{abs}\left[\mathbf{D}_1 - \mathbf{D}_2, \mathbf{D}_2 - \mathbf{D}_3, \mathbf{D}_1 - \mathbf{D}_3\right])$
  $\hat{\theta}_k = \mathrm{mean}\left[\mathbf{D}_1(\mathrm{ind_k}), \mathbf{D}_2(\mathrm{ind_k}), \mathbf{D}_3(\mathrm{ind_k})\right]$
end

IV. Numerical Results

We consider a coprime FoV array, as shown in Fig. 2, which consists of 11 elements and has the same aperture as a ULA containing 30 elements with half-wavelength element spacing. There are total $L = 400$ snapshots. As shown in Fig. 2 (b), the first group of subarray sets has $\Delta_1 = 5.5\lambda$, corresponding to visible region of $[-5.21^\circ,\ 5.21^\circ]$. The second one, shown in Fig. 2 (c), has $\Delta_2 = 4\lambda$, corresponding to visible region of $[-7.18^\circ,\ 7.18^\circ]$. The last one, shown in Fig. 2 (d), has $\Delta_3 = 1.5\lambda$, corresponding to visible region of $[-19.47^\circ,\ 19.47^\circ]$.

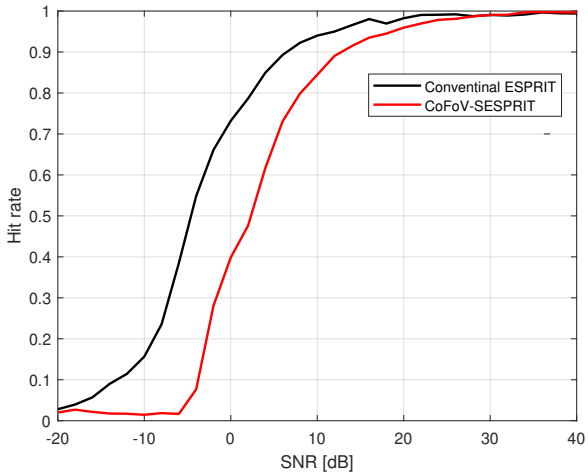

(a)

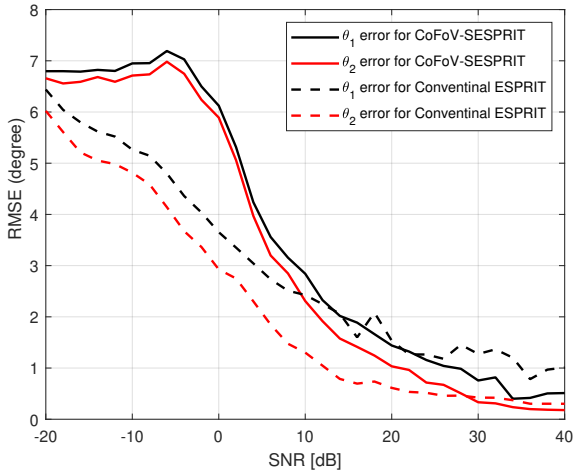

(b)

Fig. 3. (a-b) Hit rate and RMSE comparison with $\Delta_\theta = 9.29^\circ$.

To evaluate the DoA estimation performance of the CoFoV-SESPRIT, we apply the hit or missing criterion [30] to examine the DoA estimation successful rate under different input SNR values. Here, a hit denotes that the absolute error of the estimated DoA is within the 3-dB bandwidth angular resolution. For comparison, we also show the estimation hit rate of the classical ESPRIT on ULA with 11 elements and element spacing of half wavelength. The ULA with 11 elements has

3-dB beamwidth of $\Delta_\theta = 9.29°$. We placed two targets with normalized reflection coefficients of $s_1 = 1$ and $s_2 = 1$, which remain unchanged during the processing interval. One angle is drawn uniformly at random from $[-90°, 90°]$, and the second angle is separated by a value Δ_θ chosen from $[9.29°, 2°]$. For each input SNR selected from 13 uniformly-spaced values in the interval $[-20, 40]$ dB, we perform $5,000$ Monte Carlo simulations. The root-mean-squared error (RMSE), defined as $\text{RMSE} = \sqrt{\sum_{i=1}^{M_C}(\hat{\theta}_i - \theta_i)^2/M_c}$ using M_c independent trials, is used as the performance metric to measure the deviation of the estimation result $\hat{\theta}$ from the ground truth θ.

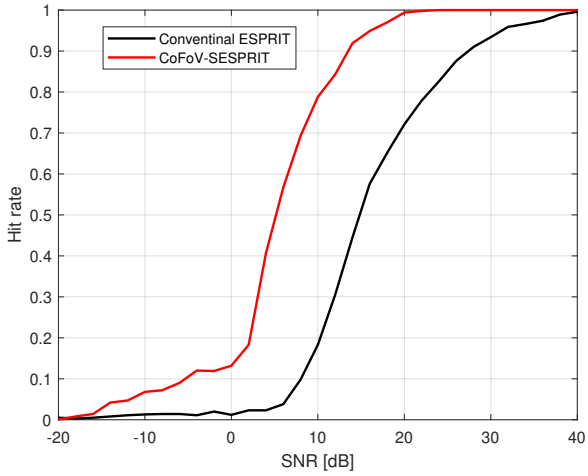

(a)

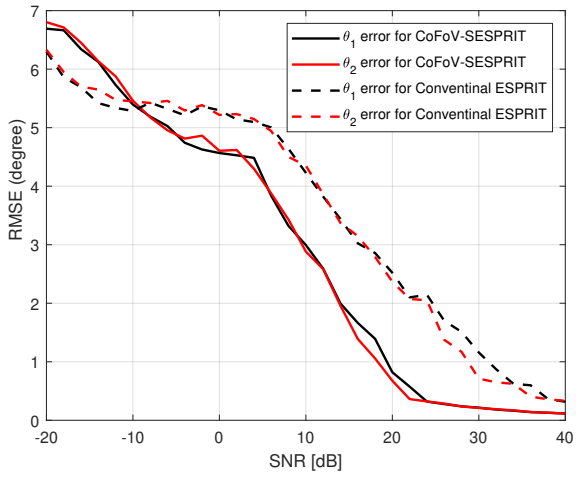

(b)

Fig. 4. (a-b) Hit rate and RMSE comparison with $\Delta_\theta = 2°$.

When angle separation is relative large, e.g., $\Delta_\theta = 9.29°$, as Fig. 3 (a)(b) shows, the performance of the CoFoV-SESPRIT is slightly worse than the conventional ESPRIT at low SNRs. This is mainly due to the angle unfolding error in the CoFoV-SESPRIT when SNRs are low. At high SNRs, the hit rate and RMSE of CoFoV-SESPRIT is close to the conventional ESPRIT.

When Δ_θ is small, e.g., $\Delta_\theta = 2°$, as shown in Fig. 4 (a)(b), the CoFoV-SESPRIT has better performance in hit rate and RMSE comparison, which is expected since the proposed SLA has a large aperture.

V. Conclusions

We developed a coprime FoV assisted angle unfolding approach for sparse ESPRIT to resolve the DoA estimation ambiguities when applying ESPRIT to general sparse linear arrays. The CoFoV-SESPRIT algorithm provides more degree-of-freedom in designing sparse linear arrays to achieve a large aperture, reducing the mutual coupling among the antenna elements and further bringing down the system cost. The simulation results demonstrated that the CoFoV-SESPRIT on SLAs has better performance in resolving spatially closed targets than conventional ESPRIT on a ULA with the same number of antenna elements. The simulation also confirmed that there is a slight performance degradation in CoFoV-SESPRIT at low SNRs due to angle unfolding errors.

References

[1] S. Tokoro, K. Kuroda, A. Kawakubo, K. Fujita, and H. Fujinami, "Electronically scanned millimiter-wave radar for precrash safety and adaptive cruise control system," in *Proc. IEEE Intelligent Vehicles Symp.*, Columbus, OH, June 2003.

[2] R. Schmidt, "Multiple emitter location and signal parameter estimation," *IEEE Trans. Antennas Propag.*, vol. 34, no. 3, pp. 276–280, 1986.

[3] A. Barabell, "Improving the resolution performance of eigenstructure-based direction-finding algorithms," in *IEEE International Conference on Acoustics, Speech, and Signal Processing*, vol. 8. IEEE, 1983, pp. 336–339.

[4] W. Liao and A. Fannjiang, "MUSIC for single-snapshot spectral estimation: Stability and super-resolution," *Applied and Computational Harmonic Analysis*, vol. 40, no. 1, pp. 33–67, 2016.

[5] R. Roy and T. Kailath, "ESPRIT-estimation of signal parameters via rotational invariance techniques," *IEEE Transactions on Acoustics, Speech, and Signal Processing*, vol. 37, no. 7, pp. 984–995, 1989.

[6] G. Xu, S. D. Silverstein, R. H. Roy, and T. Kailath, "Beamspace ESPRIT," *IEEE Transactions on Signal Processing*, vol. 42, no. 2, pp. 349–356, 1994.

[7] M. D. Zoltowski, M. Haardt, and C. P. Mathews, "Closed-form 2-D angle estimation with rectangular arrays in element space or beamspace via unitary ESPRIT," *IEEE Transactions on Signal Processing*, vol. 44, no. 2, pp. 316–328, 1996.

[8] S. Sun, A. P. Petropulu, and H. V. Poor, "MIMO radar for advanced driver-assistance systems and autonomous driving: Advantages and challenges," *IEEE Signal Processing Magazine*, vol. 37, no. 4, pp. 98–117, 2020.

[9] C. Waldschmidt, J. Hasch, and W. Menzel, "Automotive radar — From first efforts to future systems," *IEEE Journal of Microwaves*, vol. 1, no. 1, pp. 135–148, 2021.

[10] M. Markel, *Radar for Fully Autonomous Driving*. Boston, MA: Artech House, 2022.

[11] Z. Peng, C. Li, and F. Uysal, *Modern Radar for Automotive Applications*. London, UK: IET, 2022.

[12] J. Li and P. Stoica, "MIMO radar with colocated antennas," *IEEE Signal Process. Mag.*, vol. 24, no. 5, pp. 106–114, 2007.

[13] C. Schmid, R. Feger, C. Wagner, and A. Stelzer, "Design of a linear non-uniform antenna array for a 77-GHz MIMO FMCW radar," in *Proc. IEEE MTT-S Intl. Microwave Workshop on Wireless Sensing, Local Positioning, and RFID*, Cavtat, Croatia, Sept. 2009.

[14] J. Searcy and S. Alland, "MIMO antenna with elevation detection," U.S. Patent 9 541 639 B2, Jan. 10, 2017.

[15] B. Friedlander, "The root-MUSIC algorithm for direction finding with interpolated arrays," *Signal processing*, vol. 30, no. 1, pp. 15–29, 1993.

[16] S. Sun and A. P. Petropulu, "A sparse linear array approach in automotive radars using matrix completion," in *IEEE International Conference on Acoustics, Speech and Signal Processing (ICASSP)*. IEEE, 2020, pp. 8614–8618.
[17] S. Sun and Y. D. Zhang, "4D automotive radar sensing for autonomous vehicles: A sparsity-oriented approach," *IEEE Journal of Selected Topics in Signal Processing*, vol. 15, no. 4, pp. 879–891, 2021.
[18] C.-L. Liu, P. Vaidyanathan, and P. Pal, "Coprime coarray interpolation for DOA estimation via nuclear norm minimization," in *2016 IEEE International Symposium on Circuits and Systems (ISCAS)*. IEEE, 2016, pp. 2639–2642.
[19] S. Qin, Y. D. Zhang, and M. G. Amin, "Generalized coprime array configurations for direction-of-arrival estimation," *IEEE Transactions on Signal Processing*, vol. 63, no. 6, pp. 1377–1390, 2015.
[20] P. Pal and P. P. Vaidyanathan, "Nested arrays: A novel approach to array processing with enhanced degrees of freedom," *IEEE Transactions on Signal Processing*, vol. 58, no. 8, pp. 4167–4181, 2010.
[21] J. Fang, J. Li, Y. Shen, H. Li, and S. Li, "Super-resolution compressed sensing: An iterative reweighted algorithm for joint parameter learning and sparse signal recovery," *IEEE Signal Processing Letters*, vol. 21, no. 6, pp. 761–765, 2014.
[22] T. Yardibi, J. Li, P. Stoica, M. Xue, and A. B. Baggeroer, "Source localization and sensing: A nonparametric iterative adaptive approach based on weighted least squares," *IEEE Transactions on Aerospace and Electronic Systems*, vol. 46, no. 1, pp. 425–443, 2010.
[23] A. Khan, S. Wang, and Z. Zhu, "Angle-of-arrival estimation using an adaptive machine learning framework," *IEEE Communications Letters*, vol. 23, no. 2, pp. 294–297, 2018.
[24] P.-C. Chen and P. Vaidyanathan, "Rank properties of manifold matrices of sparse arrays," in *55th Asilomar Conference on Signals, Systems, and Computers*. IEEE, 2021, pp. 1628–1633.
[25] B. Ottersten, M. Viberg, and T. Kailath, "Performance analysis of the total least squares ESPRIT algorithm," *IEEE Transactions on Signal Processing*, vol. 39, no. 5, pp. 1122–1135, 1991.
[26] Z. Li and C. Alcalde, "Angle finding for a detector having a paired staggered array," Sep. 17, 2019, US Patent 10,416,680.
[27] H. Akaike, "A new look at the statistical model identification," *IEEE Trans. Acoust., Speech, Signal Process.*, vol. 37, no. 1, pp. 8–15, 1989.
[28] Y. Barron, J. Rissanen, and B. Yu, "The minimum description length principle in coding and modeling," *IEEE Trans. Inf. Theory*, vol. 44, no. 6, pp. 2743–2760, 1998.
[29] S. Kritchman and B. Nadler, "Non-parametric detection of the number of signals: Hypothesis testing and random matrix theory," *IEEE Transactions on Signal Processing*, vol. 57, no. 10, pp. 3930–3941, 2009.
[30] S. Na, K. V. Mishra, Y. Liu, Y. C. Eldar, and X. Wang, "TenDSuR: Tensor-based 4D sub-Nyquist radar," *IEEE Signal Processing Letters*, vol. 26, no. 2, pp. 237–241, 2018.